Laser ablation of tantalum, two-temperature physics and strength of melt

S I Ashitkov, P S Komarov, E V Struleva, N A Inogamov and M B Agranat

Joint Institute for High Temperatures of the Russian Academy of Sciences, Izhorskaya 13 Bldg 2, Moscow 125412, Russia

E-mail: `struleva.evgenia@yandex.ru`

23 February 2017

Abstract. Ablation of refractory metals with ultrashort laser pulses remains little-studied as opposed to other metals with a relatively low melting temperature like aluminum and gold. In this paper ablation of tantalum by femtosecond laser pulses is investigated. The results of hydrodynamic simulation of surface evolution are compared to experimental data obtained by a time-resolved interferomety method. The aspects of ablation dynamics induced by electronic pressure and acoustic tension at one- and two-temperature stages respectively are investigated theoretically and experimentally. The data on strength of tantalum liquid phase at extension rate of about 10^9 s^{-1} are presented.

PACS numbers: 62.20, 65.40.DE

Keywords: ablation, tantalum, strength of melt, femtosecond laser pulses

1. Introduction

The importance of study of laser ablation is associated with the development of novel precision technologies for processing of wide range materials, using in energetic and electronic industry, creation of nanoparticles, surface nanostructuring and etc. The fundamental interest is due to studying of physics of metastable states and the behavior of condensed matter near the theoretical ultimate strength [1–12]. At present, for many solid metals, there is extensive data on the dynamic strength in a wide range of temperatures and load durations. At the same time, the tensile strength of liquid metals is poorly understood. Recently a number of experiments in a microsecond and picosecond range has been carried out. In a submicrosecond range the spall strength of Sn, Pb and Zn in liquid state is of an order of magnitude less than at solid state [13, 14]. In the picosecond range the spall strength of liquid metals increases and could reach 30–50% of their ideal strength [15–17]. The result obtained in [16] for melted Fe indicates a decrease of its strength with the growth of temperature.

Ablation of refractory metals remains poor studied in a comparison to other metals with relatively low melting points. Tantalum is a specific high-strength metal with a high melting point of 3290 K and relatively low thermal conductivity. In this paper ablation of tantalum by femtosecond laser pulses (FLP) is investigated. The main goal was to obtain as an experimental and calculated data on strength of tantalum liquid phase depending of temperature at extremely high strain rate. The distinctions from thermomechanical ablation are theoretically considered which related to the effect of electron pressure on expansion dynamics at early stage when there is a high difference between electron and lattice temperature.

2. Theory

Hydrodynamics ablation material due to the pressure p_e of the two-temperature stage (2T spallation), is qualitatively different from the hydrodynamics of thermomechanical ablation on one-temperature stage (1T spallation). In both cases, break occurs when a tension, stretching condensed phase, exceeds its strength.

In the case of well-studied 1T thermomechanical ablation instant tensile stress profile is a superposition of two acoustic waves of a finite length, comparable to d_T; where d_T—the thickness of the heated surface layer by FLP. A first wave propagates into the volume, and a second one is reflected from the boundary with the vacuum. Both waves move with a velocity of sound c_s. The highest negative pressure is achieved at a depth, comparable with d_T at the moment $t_s = d_T/c_s$. If the value $|-p|_{\max}$ exceeds the strength, nucleation and spalling.

Let us consider a question of the 2T spalling. Electronic pressure p_e is determined by the electron temperature profile (figure 1), unlike the 1T case. Decrease of p_e occurs because of the electron conductivity and electron-ion relaxation which comes to an end in time t_{eq}. It is important that the value t_{eq} is usually substantially less than the acoustic scale t_s. In case of tantalum, the 2T hydrodynamic modeling results in the following values: during $t_{\text{eq}} \approx 7$ ps more than half of the absorbed energy goes to the ionic subsystem, the warm layer thickness is $d_T \approx 75$ nm, the acoustic time $t_s = d_T/c_s \approx 25$ ps at $c_s = 3$ km/s.

Electronic pressure reaches a maximum value in the skin layer l_{abs} to the end of the laser pulse of duration $\tau_L = 100$ fs. At the same time the following conditions are satisfied: $\tau_L \ll t_{\text{eq}} < t_s$ and $l_{\text{abs}} < d_T$. In time $t < t_{\text{eq}}$ the 2T expansion wave extends from a border with vacuum. In the 2T expansion wave substance is expanding—density decreases from the initial value ρ to the value $\rho - \Delta\rho$. The expansion has a little effect on the electronic pressure, because p_e is determined in general by the temperature T_e, and the expansion has a weak influence on the temperature due to the large thermal conductivity at 2T stage. However, the expansion strongly affects the ion pressure p_i, which varies from an initial value $p_i = 0$ to a value $p_i = -p_e$.

Thus, the substance of 1T state on binodal 1T of the equation of state $p = 0$ at 300 K is transferred first to a state of $p_e > 0$, $p_i \approx 0$, and then in a layer thickness $x = c_s t$ under the action of 2T rarefaction wave, a substance changes its state to 2T binodal of 2T state equation with zero total the pressure $p = p_e + p_i = 0$ in the condensed phase. The 2T rarefaction wave matter moves at a speed of:

$$u \approx c_s \frac{\Delta\rho}{\rho} \approx \frac{p_e c_s}{K} = A\left(\frac{p_e}{10GPa}\right)[m/s], \qquad (1)$$

The value $A = 170$ m/(s GPa), $K = 200$ GPa

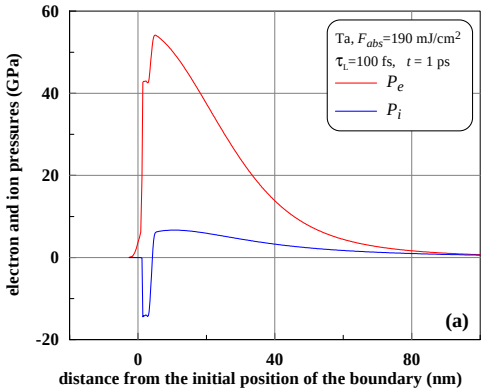

Figure 1. Profiles of partial pressures p_e and p_i in the surface layer of tantalum after 1 ps after exposure to FLI; $\tau_L = 100$ fs, $F^{\text{abs}} = 190$ mJ/cm^2.

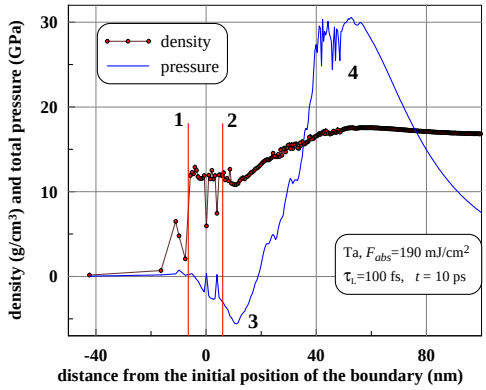

Figure 2. Profiles of density (black line) and total pressure p (blue line) on the time interval between 2T and 1T stages.

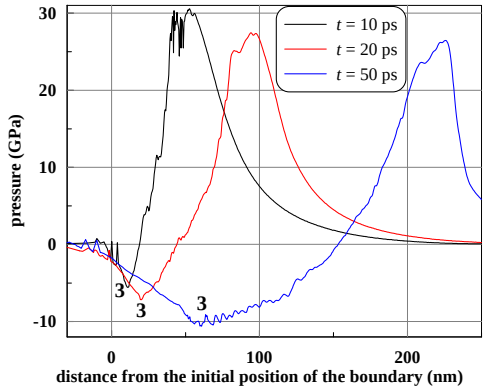

Figure 3. Calculated profiles of total pressure on the 1T stage after 10, 20, and 50 ps after exposure to FLI; $\tau_L = 100$ fs, $F^{\text{abs}} = 190$ mJ/cm^2.

of the volume compressibility module at room temperature is taken here for evaluation.

Call this layer u-layer. Acceleration of substance in u-layer occurs due to the reset of the total pressure $p = p_e + p_i$ value of $p \approx p_e$ to a value equal to zero. For 2T spalling the following is important. Reducing the electronic pressure p_e over time is determined by the spread of electronic heat from the skin layer to the heated layer of thickness d_T and by the heat transfer into the ionic subsystem. As a result, at times t, smaller than t_{eq}, pressure p_e repeatedly decreases. Thus, in case of a sufficiently rapid fall of pressure p_e $p_e/|\dot{p}_e| < t$, the area of high tensile stresses between u-layer and the rest of the material is formed. In this zone the value $|p_i|$ increases compared to the values $|p_i|$ in the u-layer. If higher values $|p_i|$ exceed the strength of the condensed phase, the nucleation begins.

Thus, if in 1T spalling the surface layer of high pressure p and thickness d_T plays an important role, in the case of 2T spalling the inhibition of u-layer due to the rapid time drop of electronic pressure p_e plays the similar role. It is necessary that the pressure p_e fell faster than the time that sound takes to run across u-layer. Figure 2 shows a transitional situation between 2T stage and 1T stage 10 ps after the femtosecond laser pulse action. Dips in the density and corresponding values $p = 0$ relate to places where gaps were formed in the u-layer in the condensed phase at the stage 2T. Plot relating to u-layer is between marks 1 and 2. Its outer part moves inertially at high speed around 2 km/s.

To the right of the mark 2 in figure 2 a wave is moving that consists of a compression section 4 which is followed by the section of underpressure with a minimum at 3.

This wave is standardly formed as a result of thermomechanical action of an ultrashort laser pulse (see., for example, [7–11]). Further extension of the wave 3-4 in the target volume at the stage 1T is shown in the figure 3.

The area of negative pressure p^- a minimum of 3 is deepening gradually (figure 3). The process of deepening of the area p^- ends by 40–50 ps at a depth of approximately 50 nm from the boundary with a vacuum and then its depth varies slightly. At 40–50 ps minimum of p^- leaves the melt layer of 50 nm thick. From figure 3, for example, follows that if the strength of the condensed state is 7 GPa, according to the calculation, the fracture should occur about 30 ps at about 40 nm in the melt. If the strength is less, cavitation occurs in the melt at a smaller depth and shorter times. This is characteristic of thermomechanical ablation of metals (1T-spalling) by femtosecond laser pulse.

3. Experiment

For investigation of the dynamics of the ablation layer chirped pulse interferometry technique was applied. This technique allows a continuous recording of both amplitude and phase of the reflected diagnostic wave as a function of time in the picosecond range with spatial

and temporal resolution. Method is based on the fact that the various spectral components of the diagnostic pulse probed the target at different times.

The radiation source was CPA (chirped pulse amplification) Ti:sapphire system generating pulses at a central wavelength of $\lambda_0 = 800$ nm and $\Delta\lambda = \pm 20$ nm spectral wide. Powerful pump pulse with duration of 40 fs heated the target. For probing chirped pulse with duration of 300 ps was used. For diagnostics a Michelson interferometer in imaging configuration coupled with a diffraction spectrometer Solar MS3504i (Czerny–Turner scheme) was used. The interferograms were recorded by camera SensiCam QE. The used scheme of measurement provides a continuous registration process dynamics with the temporal resolution of $\delta t \approx 2$ ps in the time interval $\Delta t = 0$–200 ps. The spatial resolution in the target plane was about 2 μm. For the processing of two-dimensional interferograms Fourier analysis was applied. The accuracy of phase shift measurement was $\delta\varphi \approx 0.01$ rad, which corresponds to the error in determining the value of the surface displacement at $\delta z \leq 1 \div 2$ nm. The experimental scheme was described in detail in [17].

An experimental sample was tantalum film of 0.6 μm in thickness deposited on the polished glass substrate. Pump radiation of p-polarization was focusing on the target at an angle of incidence of 60° by the lens with a focal length of 30 cm in a spot with a Gaussian distribution and a radius of 25 μm on the level of e^{-1}. Energy of pump E was measured with a calibrated photodiode. In addition calorimeter Sigma (Coherent) measured the energy of the reflected pulse E_r, in order to determine a value of an integral reflection coefficient $R_L = E_r/E$. The measured ablation threshold of Ta target for the incident fluence was equal $F_a \approx 0.31$ J/cm^2. Its value is determined from the dependence of a transverse dimension of crater on pump energy E [18]. Near the ablation threshold the value of the laser reflectance was $R_L \approx 0.38$. Correspondently, the magnitude of the ablation threshold on the absorbed fluence was $F_a^{\text{abs}} = (1 - R)F_a \approx 0.19$ J/cm^2.

The characteristic profile of the ablation crater and the spatial distribution of the radiation on the target are shown in figure 4. The displacement accuracy of $\delta h \approx 1$ nm, measured as root mean square values of displacement over an unperturbed area (figure 4), indicates that surface deformations a small as 1 nm can be detected.

The measured depth of the crater was about $h \approx 22$ nm. In spite of the Gaussian profile of the laser beam, the crater has a flat top shape. This indicates clearly expressed threshold character of the ablation process. Also we can see the absence of a second

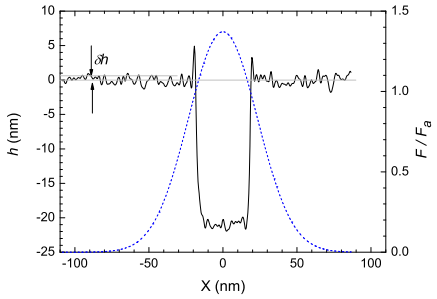

Figure 4. Profile of ablation crater on sample surface of tantalum with $F_0 = 1.4F_a$ (solid line); spatial distribution of the energy density on the target (dotted line).

smaller crater whth the depth of a few nanometers or less, which should be the result of ablation of material by electronic pressure p_e. It follows that the threshold of this process is a higher than the value of the threshold of thermomechanical ablation, or a very thin layer of material may be removed (comparable or less that the error $d \leq \delta h$).

Figure 5 shows the dynamics of the movement of the sample boundary. Several profiles of the induced phase changes $\Delta\varphi(t)$ of probe as a function of time was measured at different fluences of pump at the range $F/F_{\text{abl}} = 0.3$–1.1. Profiles are plotted for different distances from the center of the focal spot and corresponded to different energy density F.

The measured phase shift may be called as a change in optical properties of the material and displacement of the sample surface. At figure 5, the initial sharp jump of phase $\Delta\varphi_{\text{opt}} \approx 0.13$ rad occurs in about 4–5 ps. Rapid change φ on the picosecond scale comparable with t_ei obviously may be associated with the heating and melting of the surface layer of tantalum. Note that melting of metals under action of femtosecond laser pulses has homogeneous nature and occurs at times of $\sim 10^{-12}$–10^{-11}, comparable with t_{ei} [19].

Also to observed rapid phase jump at time scale $t < t_{\text{ei}}$ can contribute the movement of the boundaries under the action of electron pressure (2T ablation). However, in this case, the thickness of 2T ablative layer is much smaller than the probing depth ($\delta = \lambda/4\pi k \approx 20$ nm [20]) and its influence on the phase change can be neglected. Subsequent gradual changes of phase at $t \geq 8$ ps obviously connected with the beginning of the movement of melt. The character of curves $\Delta\varphi(t)$ on figure 5 allows us to split an optical stage $\Delta\varphi_{\text{opt}}(t)$ and the stage of the hydrodynamic motion $z(t)$:

$$z(t) = \frac{((\Delta\varphi(t) - \Delta\varphi_{\text{opt}}(t))\lambda}{4\pi}, \qquad (2)$$

Here we assume that the optical component $\Delta\varphi_{\text{opt}}(t)$ changes dramatically within the first 6–8 ps

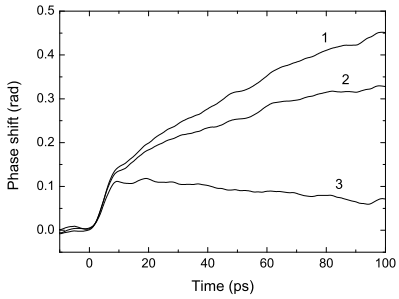

Figure 5. Temporal dynamics of phase changes $\Delta\varphi(t)$ at different energy densities FLI: 1—$F/F_{\rm abl} = 1.1$; 2—$F/F_{\rm abl} = 1.0$; 3—$F/F_{\rm abl} = 0.2$.

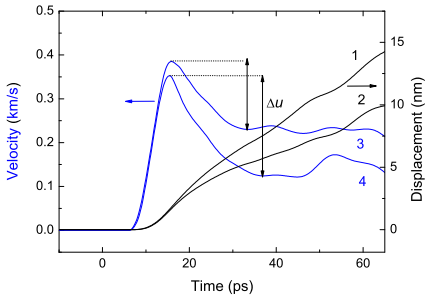

Figure 6. Wave displacement (1 and 2) and velocity (3 and 4) profiles at different energy density: 1 and 3—$F/F_{\rm abl} = 1.1$; 2 and 4—$F/F_{\rm abl} = 1.0$.

due to heating and melting the surface layer and further doesn't change in the detected range 0–200 ps because crystallization of melt occurs at the time scale $\geq 10^{-9}$ s. The velocity profiles $u(t)$ in figure 6 were obtained by the differentiating the smoothed profile $z(t)$, extracted from the dependency $\Delta\varphi(t)$ (Figure 5) taking into account (2). The maximum velocity $u_{\max}$ is achieved about $t_1 \approx 10$ ps after a start of the movement. Acceleration of layer is due to pressure gradient into the heated layer of thickness d_T.

The subsequent decline of the velocity is due to a decrease in the pressure gradient, and to resistance to the action on a substance of tensile stresses σ. If the value of tensile stress exceeds the strength of the condensed state $\sigma_{\rm liq}$, cavitation process is developed into stretched melt, that leads to it's discontinuity and separation of ablative layer. As well the measurements in shock wave experiments [21], tensile strength of the condensed state $\sigma_{\rm liq}$ can be estimated from the relation:

$$\sigma_{\rm liq} = \rho_{\rm liq} c_{\rm liq} \Delta u/2, \tag{3}$$

Here $\rho_{\rm liq} = 8.13$ g/cm^3, $c_{\rm liq} = 2.9$ km/s are density and sound velocity in the melt respectively according to an equation of state [22]. The measured values of the pull back velocity Δu are equal to 0.23 km/s at $F \approx F_a$ and 0.16 km/s at $F \approx 1.1F_a$ (Figure 6).

The corresponding values $\sigma_{\rm liq}$ of liquid tantalum according to (3) are 4.6 and 3.2 GPa. The results show a rapid decrease of the strength of melt with increasing temperature. The growth of F by 10% leads to drop of strength by 30%. The estimated strain rate by the expression [21]:

$$\dot{\varepsilon} = \frac{\Delta u}{\Delta t}\frac{1}{2c}, \tag{4}$$

gives the value $\dot{\varepsilon} \sim 10^9$ s^{-1}. Here $\Delta t = t_{\min} - t_{\max}$, where $t_{\max}$ and $t_{\min}$ are the times corresponding the maximum and minimum velocity value $u(t)$.

Near the threshold F_a the depth at which nucleation occurs in the melt is approximately equal to the thickness of the spall plate, which is estimated from the ratio of $L_{\rm abl} = c_{\rm liq}(t_{\max} - t_{\min})/2 \approx 30$ nm. The estimated value $L_{\rm abl}$ agrees well with the depth of ablation crater near the threshold: $h \approx 25$ nm (Figure 4). Note that the results measurements of the strength and thickness of spall layer in vicinity of ablation threshold are in good agreement with the data of calculating tensile stress (Figure 3) in case of thermomechanical ablation.

4. Conclusions

Femtosecond laser ablation of tantalum is examined theoretically and experimentally. The results of 2T hydrodynamic simulation indicate two possible mechanisms. Ablation of a thin layer of several nanometers in thickness during first picoseconds at 2T stage could be induced by fast reduction of electronic pressure. Thermomechanical ablation as a result of acoustic tension action on a liquid surface layer, cavitation in a melt and separation of a layer of several tens nanometers in thickness at about 10^{-11} s during 1T stage could be the second mechanism. The results of interferometric measurements indicate the only thermomechanical ablation. Characteristic temporal and spatial scale, including measured values of tension near ablation threshold, are in agree with simulations. Measured strength of liquid tantalum near ablation threshold indicate dramatic reduction of strength with increasing temperature. At the same time no experimental evidence of tantalum ablation due to electronic pressure under single laser pulses has been found. The reason could be surface modifications at subnanoscale that are not clearly observable by means of used diagnostics.

Acknowledgments

The experiments were performed using the scientific facility "Terawatt Femtosecond Laser Complex" of

JIHT of RAS. This work was supported by the Russian Science Foundation, grant No. 14-50-00124.

References

[1] Kanel G I, Zaretsky E B, Razorenov S I, Ashitkov S I and Fortov V E 2017 *Phys. Usp.* **60** 490
[2] Ashitkov S I, Agranat M B, Kanel G I, Komarov P S and Fortov V E 2010 *JETP Lett.* **92** 516
[3] Whitley V H, McGrane S D, Eakins D E, Bolme C A, Moore D S and Bingert J F 2011 *Appl. Phys.* **109** 013505
[4] Crowhurst J C, Armstrong M R, Knight K B, Zaug J M and M B E 2011 *Phys. Rev. Lett.* **107** 144302
[5] Abrosimov S A, Bazhulin A P, Voronov V V, Geras'kin A A, Krasyuk I K, Pashinin P P, Semenov A Y, Stuchebryukhov I A, Khishchenko K V and Fortov V E 2013 *Quantum Electron.* **43** 246
[6] Krasyuk I K, Pashinin P P, Semenov A Y, Khishchenko K V and Fortov V E 2016 *Laser Phys.* **26** 094001
[7] Ivanov D and Zhigilei L 2003 *Phys. Rev.* B **68** 064114
[8] Bulgakova N, Stoian R, Rosenfeld A, Hertel I and Campbell E 2004 *Phys. Rev.* B **69** 054102
[9] Agranat M, Anisimov S, Ashitkov S, Zhakhovskii V, Inogamov N, Nishihara K, Petrov Y, Khokhlov V and Fortov V 2007 *Appl. Surf. Sci.* **253** 6276
[10] Povarnitsyn M, Itina T, Sentis M, Khishchenko K and Levashov P 2007 *Phys. Rev.* B **75** 235414
[11] Inogamov N A, Zhakhovskii V V, Ashitkov S I, Petrov Y, Agranat M, Anisimov S, Nishihara K and Fortov V 2008 *J. Exp. Theor. Phys.* **107** 1
[12] Starikov S V, Stegailov V V, Norman G E, Fortov V E, Ishino M, Tanaka M, Hasegawa N, Nishikino M, Ohba T, Kaihori T, Ochi E I T, Kavachi T, Tamotsu S, Pikuz T A, Skobelev I Y and Faenov A Y 2011 *JETP Lett.* **93** 719
[13] Kanel G, Savinykh A, Garkushin G and Razorenov S 2015 *JETP Lett.* **102** 548
[14] Zaretsky E B 2016 *J. Appl. Phys.* **120** 025902
[15] Ashitkov S I, Komarov P S, Ovchinnikov A V, Struleva E V and Agranat M B 2016 *JETP Lett.* **103** 544
[16] Struleva E V, Ashitkov S I, Komarov P S, Khishchenko K V and Agranat M B 2016 *J. Phys.: Conf. Ser.* **774** 012098
[17] Ashitkov S I, Komarov P S, Ovchinnikov A V, Struleva E V, Zhakhovskii V V, Inogamov N A and Agranat M B 2014 *Quantum Electron.* **44** 535
[18] Liu J 1982 *Opt. Lett.* **7** 196
[19] Rethfeld B, Temnov V V, Sokolowski-Tinten K, Tsu P, von der Linde D, Anisimov S I, Ashitkov S I and Agranat M B 2004 *J. Opt. Technol.* **71** 348
[20] Ashitkov S I, Komarov P S, Struleva E V, Yurkevich A A, and Agranat M B 2016 *High Temp.* **54** 899
[21] Kanel G 2010 *Int. J. Fract.* **163** 173
[22] Fortov V, Khishchenko K, Levashov P and Lomonosov I 1998 *Nucl. Instr. Meth. Phys. Res. A* **415** 604